Preprints of the 21st IFAC World Congress (Virtual)
Berlin, Germany, July 12-17, 2020

Constrained Linear State Signal Shaping Model Predictive Control for Harmonic Compensation in Power Systems *

Kathrin Weihe * **Carlos Cateriano Yáñez** *,**,***
Georg Pangalos *** **Gerwald Lichtenberg** *

* *Hamburg University of Applied Sciences, Faculty Life Sciences, Germany (e-mail: kathrin.weihe@haw-hamburg.de, carlos.caterianoyanez@haw-hamburg.de, gerwald.lichtenberg@haw-hamburg.de)*
** *Instituto U. de Automática e Informática Industrial, Universitat Politècnica de València, Spain.*
*** *Fraunhofer Institute for Silicon Technology, Germany (e-mail: georg.pangalos@isit.fraunhofer.de).*

Abstract: For signal shaping problems, in contrast to reference following problems, a possibility is to make use of the signal's shape as a control objective, described by a difference equation. In order to do this, a shape class is defined, giving a measure of how close to a specific shape a signal is. The shape class defines the weighting matrices of the standard quadratic cost function of a model predictive controller. The optimization problem is solved with constraints using a standard quadratic program solver. An application example shows the suitability of the approach for active power filters.

Keywords: Predictive control, optimal control theory, optimal operation and control of power systems, modeling and simulation of power systems, control system design.

1. INTRODUCTION

Predicting the output of a system by using a model is the key to model predictive control (MPC). With the increasing computational power, the use of MPC algorithms is suitable for an increasing number of applications where specific references are to be followed. If a linear model of the plant is available and the control goal can be expressed as a quadratic cost function possibly with linear equality and inequality constraints, the MPC problem results in a numerically efficient solvable convex optimization problem, Maciejowski (2002). This class of problems can be solved using standard quadratic problem (QP) solvers, which are available online, e.g. Stellato et al. (2017).

The classical parameter setting for MPC algorithms is to use only entries on the diagonal of the weighting matrices and a specific reference over time. The weightings represent the importance of the defined criteria for a given point in time within the prediction horizon. The final state of the controlled system, e.g. the shape of a formation, a sheet or a voltage, however, might be reached faster or more accurately on a different path. Thus in some applications the exact timing is not of interest but a specific shape needs to be met, e.g. formation control of multiple robots, the formation needs to be reached but the individual tracks are not of interest, see Egerstedt and Hu (2001) or in process engineering wherein sheet forming only the final shape is of interest, see Lu et al. (2016). In power electronics and electrical grids, maintaining the shape of voltages and currents is of special interest for harmonics suppression which can be done using active power filters, Kumar and Mishra (2016). Here again, the path to a harmonic free signal is of no interest but a specific shape needs to be tracked. In other words, a sinusoidal shape of a signal has to be forced, but the phase is not of interest. Of special interest for this application example is the harmonic shape class, basically giving a measure on how sinusoidal a signal's shape is.

In the area of signal processing, problems of this kind are well known and often referred to as signal shaping, see e.g. Brandonisio and Kennedy (2014).

The equivalence of signal shaping problems using a representation of the desired shape by linear difference equations in terms of the state variables and standard MPC problems with quadratic cost functions was shown in Cateriano Yáñez et al. (2018). In a recently published application paper, a state signal shaping MPC has been compared to a classical control scheme, showing promising results, see Weihe et al. (2018).

Even though the controller proposed in Cateriano Yáñez et al. (2018); Weihe et al. (2018) managed to impose a sinusoidal shape with the right frequency, the amplitude was not under control, leading to unstable scenarios. This contribution extends this approach by including constraints in the optimization problem to address this shortcoming.

* This contribution was partly developed within the project NEW 4.0 (North German Energy Transition 4.0) which is funded by the German Federal Ministry for Economic Affairs and Energy (BMWI).

This paper is organized as follows: Section 2 introduces the linear shape class and the harmonic shape class. Section 3 starts with the definition of a state-space model, defines the constrained MPC problem, and integrates the shape class into the MPC problem by introducing the pattern band matrix. In Section 4, an application example in the field of power quality compensation for renewable energy grid integration is presented. Finally, section 5 gives a summary and draws conclusions.

2. SHAPE CLASS

This section introduces the shape class as a tool to compare an arbitrary discrete-time signal to a given signal shape.

Considering a discrete-time state signal of a system with n states, the set

$$\mathscr{X}_{\mathbf{V}}=\left\{\mathbf{x}(1),\mathbf{x}(2),\ldots \middle| \mathbf{V}\begin{pmatrix}\mathbf{x}(k+1)\\ \vdots \\ \mathbf{x}(k+T)\end{pmatrix}=\mathbf{0}\;\forall k=0,1,\ldots\right\}, \quad (1)$$

is introduced as a shape class, where $\mathbf{x}\in\mathbb{R}^n$ denotes the state vector and $\mathbf{V}\in\mathbb{R}^{s\times nT}$ denotes the shape matrix for T consecutive states, with a number of s linear difference equations that take part in the state shape analysis as introduced in Cateriano Yáñez et al. (2018). This set denotes consecutive states, that are mapped to the zero vector by a linear map, thus it is also referred to as the kernel of the shape. The goal of a shape analysis is to find the kernel for a given shape matrix or to find a set in the neighborhood of the kernel. If the shape analysis, i.e. the multiplication of the shape matrix with a state vector, yields a vector different from the zero vector, this vector is referred to as shape residual. To evaluate how good a state sequence matches a given signal shape, the Euclidean norm of the shape residual

$$\parallel \mathbf{V}\mathbf{X}(k)\parallel_2 \quad (2)$$

is used, where $\mathbf{X}(k)=(\mathbf{x}(k+1),\mathbf{x}(k+2),\ldots,\mathbf{x}(k+T))^\intercal$. Note that any shape that can be described as a linear difference equation can be used for shape analysis.

3. LINEAR STATE SIGNAL SHAPING

Using shape classes, not only shape analysis is possible, but also controlling plant outputs or states to assume a given shape using MPC. This concept is called linear state signal shaping (LS^3). This section discusses how to incorporate shape classes into the MPC scheme.

3.1 Constrained Model Predictive Control

Consider a linear discrete-time state space model

$$\mathbf{x}(k+1)=\mathbf{A}\mathbf{x}(k)+\mathbf{B}\mathbf{u}(k), \quad (3)$$
$$\mathbf{x}(0)=\mathbf{x}_0, \quad (4)$$

with n states, m inputs and the initial state $\mathbf{x}_0$, input vector $\mathbf{u}\in\mathbb{R}^m$, where $\mathbf{A}\in\mathbb{R}^{n\times b}$ denotes the system matrix and $\mathbf{B}\in\mathbb{R}^{n\times m}$ denotes the input matrix. The optimal control action leading the states to the equilibrium can be obtained by a finite-time linear quadratic regulator (LQR), which minimizes the cost function

$$\mathbf{J}(\mathbf{x},\mathbf{u})=\sum_{k=0}^{N-1}\left(\mathbf{x}(k)^\intercal\mathbf{Q}_k\mathbf{x}(k)+\mathbf{u}(k)^\intercal\mathbf{R}_k\mathbf{u}(k)\right)\;, \quad (5)$$

where $\mathbf{Q}_k\in\mathbb{R}^{n\times n}\succeq 0$ denotes the state cost weighting matrix for all states at time step k and $\mathbf{R}\in\mathbb{R}_k^{m\times m}\succ 0$ denotes the input cost weighting matrix , for the discrete-time horizon N. In constrained MPC, the LQR cost function is minimized by formulating the problem as a quadratic program (QP)

$$\begin{aligned}
\min_{\mathbf{x},\mathbf{u}}\quad & \sum_{k=0}^{H_p-1}\mathbf{x}(k)^\intercal\mathbf{Q}_k\mathbf{x}(k)+\sum_{k=1}^{H_u}\mathbf{u}(k)^\intercal\mathbf{R}_k\mathbf{u}(k) && (6a)\\
\text{subject to}\quad & \mathbf{x}(k+1)=\mathbf{A}\mathbf{x}(k)+\mathbf{B}\mathbf{u}(k) && (6b)\\
& \mathbf{x}(0)=\mathbf{x}_0 && (6c)\\
& \underline{\mathbf{x}}\le\mathbf{x}(k)\le\overline{\mathbf{x}} && (6d)\\
& \underline{\mathbf{u}}\le\mathbf{u}(k)\le\overline{\mathbf{u}}\;, && (6e)
\end{aligned}$$

where H_p is called prediction horizon and H_u is called input horizon, $\underline{\mathbf{x}}$ and $\underline{\mathbf{u}}$ denote the lower state and input bounds, and $\overline{\mathbf{x}}$ and $\overline{\mathbf{u}}$ denote the upper state and input bounds.

The QP can be solved using standard solvers by defining a decision variable $\mathbf{z}=\begin{pmatrix}\mathbf{X}_{H_p} & \mathbf{U}_{H_u}\end{pmatrix}^\intercal\in\mathbb{R}^{nH_p+mH_u}$ with $\mathbf{X}_{H_p}=\begin{pmatrix}\mathbf{x}(0) & \mathbf{x}(1) & \ldots & \mathbf{x}(H_p-1)\end{pmatrix}^\intercal$ as well as $\mathbf{U}_{H_u}=\begin{pmatrix}\mathbf{u}(1) & \mathbf{u}(2) & \ldots & \mathbf{u}(H_u)\end{pmatrix}^\intercal$ and reformulating (6) as

$$\begin{aligned}
\min_{\mathbf{z}}\quad & \frac{1}{2}\mathbf{z}^\intercal\mathbf{P}\mathbf{z} && (7a)\\
\text{subject to}\quad & \mathbf{F}\mathbf{z}=\mathbf{c} && (7b)\\
& \underline{\mathbf{z}}\le\mathbf{z}\le\overline{\mathbf{z}}\;, && (7c)
\end{aligned}$$

with appropriate matrices

$$\tilde{\mathbf{Q}}=\begin{pmatrix}\mathbf{Q}_0 & \cdots & \mathbf{0}\\ \vdots & \ddots & \vdots\\ \mathbf{0} & \cdots & \mathbf{Q}_{H_p-1}\end{pmatrix}, \quad (8)$$

$$\tilde{\mathbf{R}}=\begin{pmatrix}\mathbf{R}_1 & \cdots & \mathbf{0}\\ \vdots & \ddots & \vdots\\ \mathbf{0} & \cdots & \mathbf{R}_{H_u}\end{pmatrix}, \quad (9)$$

$$\mathbf{P}=\begin{pmatrix}\mathbf{0}^{n\times n} & \mathbf{0} & \mathbf{0}\\ \mathbf{0} & \tilde{\mathbf{Q}} & \mathbf{0}\\ \mathbf{0} & \mathbf{0} & \tilde{\mathbf{R}}\end{pmatrix}, \quad (10)$$

$$\mathbf{F}=\begin{pmatrix}\hat{\mathbf{A}} & \hat{\mathbf{B}}\end{pmatrix} \quad (11)$$

with

$$\hat{\mathbf{A}}=\begin{pmatrix}-\mathbf{I}^{n\times n} & \mathbf{0} & \mathbf{0} & \mathbf{0}\\ \mathbf{A} & -\mathbf{I} & \mathbf{0} & \mathbf{0}\\ \mathbf{0} & \mathbf{A} & -\mathbf{I} & \mathbf{0}\\ \mathbf{0} & \mathbf{0} & \mathbf{0} & \ddots\end{pmatrix},\hat{\mathbf{B}}=\begin{pmatrix}\mathbf{0}^{1\times H_p}\\ \mathbf{I}^{H_p}\end{pmatrix}\otimes\mathbf{B}, \quad (12)$$

and vector

$$\mathbf{c}=\begin{pmatrix}-\mathbf{A}\mathbf{x}_0\\ \mathbf{0}\\ \mathbf{0}\\ \vdots\end{pmatrix}, \quad (13)$$

where $\underline{\mathbf{z}}$ and $\overline{\mathbf{z}}$ denote the lower and upper bounds of the decision variable vector and with the matrix $\mathbf{P}$ denoting the Hessian of the optimization problem. Note that typically the Hessian is a diagonal matrix. Since in this formulation of the MPC optimization the Hessian is sparse in nature, this problem formulation is sometimes referred to as sparse formulation, Jerez et al. (2012).

For some applications, calculating the optimal changes to the input $\Delta\mathbf{U}=(\Delta\mathbf{u}(k)\;\Delta\mathbf{u}(k+1)\;\ldots\Delta\mathbf{u}(k+H_u))$ can lead to better closed loop control results in contrast to calculating the optimal input itself. For this approach, the future states can be eliminated from the decision variables of the optimization problem by formulating them as a function of future inputs and the initial state, Maciejowski (2002). For this, problem (6) is formulated as

$$\min_{\Delta\mathbf{U}} \quad \frac{1}{2}\Delta\mathbf{U}(k)\mathbf{P}\Delta\mathbf{U}(k) + \mathbf{q}^{\intercal}\Delta\mathbf{U}(k) \tag{14a}$$

$$\text{subject to} \quad \mathbf{l} \leq \boldsymbol{\Theta}\Delta\mathbf{U}(k) \leq \mathbf{o}\ , \tag{14b}$$

where $\mathbf{l} \in \mathbb{R}^{nH_p}$ denotes the lower bound of the inequality and $\mathbf{o} \in \mathbb{R}^{nH_p}$ denotes the upper bound of the inequality, and

$$\boldsymbol{\Theta} = \begin{pmatrix} \mathbf{B} & \mathbf{0} & \mathbf{0} & \cdots & \mathbf{0} \\ \mathbf{AB}+\mathbf{B} & \mathbf{B} & \mathbf{0} & \cdots & \mathbf{0} \\ \vdots & \vdots & \vdots & \ddots & \vdots \\ \sum_{j=0}^{H_p-1}\mathbf{A}^j\mathbf{B} & \sum_{j=0}^{H_p-2}\mathbf{A}^j\mathbf{B} & \cdots & \cdots & \sum_{j=0}^{H_p-H_u}\mathbf{A}^j\mathbf{B} \end{pmatrix}, \tag{15}$$

$$\boldsymbol{\Psi} = \begin{pmatrix} \mathbf{A} \\ \mathbf{A}^2 \\ \vdots \\ \mathbf{A}^{H_p} \end{pmatrix}, \tag{16}$$

$$\boldsymbol{\Upsilon} = \begin{pmatrix} \mathbf{B} \\ \mathbf{AB}+\mathbf{B} \\ \vdots \\ \sum_{j=0}^{H_p-1}\mathbf{A}^j\mathbf{B} \end{pmatrix}, \tag{17}$$

$$\mathbf{P} = \boldsymbol{\Theta}^{\intercal}\tilde{\mathbf{Q}}\boldsymbol{\Theta} + \tilde{\mathbf{R}}, \tag{18}$$

$$\mathbf{q} = -2\boldsymbol{\Theta}^{\intercal}\tilde{\mathbf{Q}}(\boldsymbol{\Psi}\mathbf{x}(k) + \boldsymbol{\Upsilon}\mathbf{u}(k-1))\ . \tag{19}$$

The Hessian (18) does not contain zeros, therefore this formulation is also referred to as dense or condensed formulation.

Using the receding horizon (RHC) strategy, only the first optimal input is applied to the plant, the resulting output or state is measured and the optimization problem is solved again with the updated initial state and a shifted prediction horizon.

3.2 Pattern Band Shape Matrix

While the resemblance of a signal with a shape can be calculated with (2), it is possible to calculate a state sequence, which matches a given shape as close as possible with

$$\min_{\mathbf{X}} \left(\mathbf{V}\mathbf{X}(k)\right)^2\ . \tag{20}$$

This only works for T consecutive states as defined in the shape class, though it is possible to extend the problem to longer state sequences by slicing the shape matrix into parts

$$\mathbf{V}_j = \mathbf{V}\begin{pmatrix} \mathbf{0}^{n(j-1)\times n} \\ \mathbf{I}^{n\times n} \\ \mathbf{0}^{n(T-j)\times n} \end{pmatrix} \text{ for } j = 1, 2, \ldots, T\ , \tag{21}$$

where each $\mathbf{V}_j \in \mathbb{R}^{s\times n}$, so that

$$\mathbf{P}_V = \begin{pmatrix} \mathbf{V}_1 & \mathbf{V}_2 & \cdots & \mathbf{V}_T & \mathbf{0} & \cdots & \mathbf{0} \\ \mathbf{0} & \mathbf{V}_1 & \mathbf{V}_2 & \cdots & \mathbf{V}_T & \ddots & \vdots \\ \vdots & \ddots & \ddots & \ddots & \ddots & \ddots & \mathbf{0} \\ \mathbf{0} & \cdots & \mathbf{0} & \mathbf{V}_1 & \mathbf{V}_2 & \cdots & \mathbf{V}_T \end{pmatrix} \in \mathbb{R}^{p_1\times p_2}, \tag{22}$$

where $p_1 = s(H_p - T + 1)$ and $p_2 = nH_p$. This allows the formulation of a minimization problem

$$\min_{\mathbf{X}_{H_p}} \left(\mathbf{X}_{H_p}^{\intercal}\mathbf{P}_V^{\intercal}\mathbf{P}_V\mathbf{X}_{H_p}\right) \tag{23}$$

for finding a shape-matching state sequence up to the prediction horizon H_p. By defining $\mathbf{Q}_S = \mathbf{P}_V^{\intercal}\mathbf{P}_V$ and replacing $\tilde{\mathbf{Q}}$ in the Hessian (10) of the sparse or (18) and (19) of the dense optimization problem formulation, it is possible to find an optimal input that drives the states of a plant towards matching the given shape as close as possible. With this approach, the Hessian becomes non-diagonal but as long as it is still positive semidefinite, the LS^3 MPC optimization problem is solvable with standard QP solvers.

3.3 Stability

A linear MPC can achieve stability by introducing a terminal constraint, Maciejowski (2002). Assuming a feasible control sequence leading to the state $\mathbf{x}_f(k)$, for LS^{3}MPC stability could analogously be achieved when the shape residual of $\mathbf{x}_f(k+1)$ does not increase. Determining a feasible set for such a terminal constraint is a subject of current research.

4. APPLICATION EXAMPLE

Harmonics in the electrical grid cause power losses and they can damage sensitive devices. The ideal shape of supply currents and voltages is purely sinusoidal, contrary to what it is observed under scenarios with harmonic distortion. In order to eliminate harmonics, active power filters (APF) are used to inject a compensation current into a point of common coupling (PCC). As shown in Cateriano Yáñez et al. (2018), using unconstrained LS^3 MPC to compensate harmonics in the grid leads to sinusoidal currents and voltages, but with this approach, increasing or decreasing amplitudes depending on the chosen weighting factors, were a major drawback. In this section, the control of an APF based on the constrained LS^3 MPC scheme is shown to provide an application example.

4.1 System Model

As shown in Fig. 1, an equivalent single-phase circuit with transmission resistance R_1 and inductance L_1 is used to model the electric grid, a non-ideal current source i_{c0} with internal resistance R_3 is used to model an APF with a coupling resistance R_2 and a coupling inductance L_2, and a non-ideal current source i_{l0} with an internal resistance R_4 is used as nonlinear load, which introduces harmonics into the grid. In this example, v_s and i_l act as measured disturbances to the system and the controller is supposed to find the optimal compensation current i_{c0} to bring the feeder line current i_f to a sinusoidal shape.

Constraining the feeder line current to a maximum current helps to reduce transmission losses when the APF is

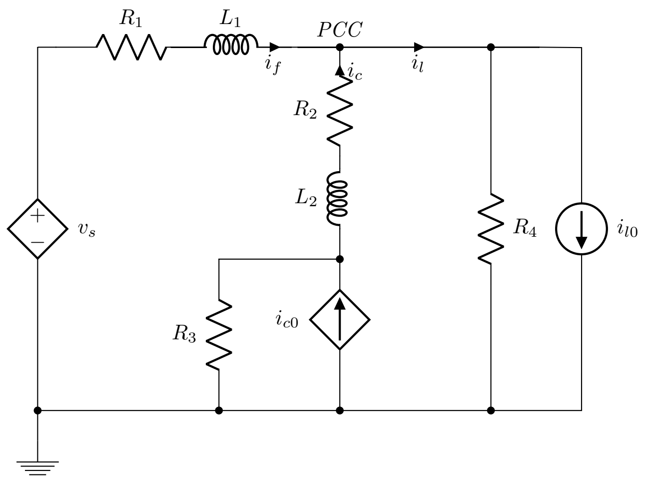

Fig. 1. Equivalent circuit of the electric grid using current sources as APF and as nonlinear load.

connected close to the nonlinear load, Fuchs and Masoum (2015).

Using Kirchhoff's current and voltage laws, the state space representation of this equivalent circuit is

$$\frac{\mathrm{d}\mathbf{x}(t)}{\mathrm{d}t} = \mathbf{A}_m\mathbf{x}(t) + \mathbf{b}_m u(t) + \mathbf{E}_m\mathbf{d}_m(t)\,, \tag{24}$$

with

$$\mathbf{A}_m = \begin{pmatrix} -\dfrac{R_1+R_4}{L_1} & -\dfrac{R_4}{L_1} \\ -\dfrac{R_4}{L_2} & -\dfrac{R_2+R_3+R_4}{L_2} \end{pmatrix}, \tag{25}$$

$$\mathbf{b}_m = \begin{pmatrix} 0 \\ \dfrac{R_3}{L_2} \end{pmatrix}, \tag{26}$$

$$\mathbf{E}_m = \begin{pmatrix} \dfrac{1}{L_1} & \dfrac{R_4}{L_1} \\ 0 & \dfrac{R_4}{L_2} \end{pmatrix}, \tag{27}$$

with the state vector $\mathbf{x}(t) = (i_f \ i_c)^\intercal$, the input $u(t) = i_{c0}$ and the vector of measured disturbances $\mathbf{d}_m(t) = (v_s \ i_{l0})^\intercal$. Since LS^3 MPC uses a discrete-time state-space representation, this continuous-time model is discretized using zero-order hold with a fixed sampling time T_s.

4.2 Harmonic Shape Class

Sinusoidal shapes are of particular interest for this example, therefore the harmonic a shape class is introduced. The property of a sine wave can be described by the differential equation

$$\frac{\mathrm{d}^2x(t)}{\mathrm{d}t^2} + \omega^2 x(t) = 0, \tag{28}$$

where ω denotes the angular frequency of the wave. To express this differential equation as shape class, it is approximated as a discrete-time difference equation using forward numerical differentiation

$$\ddot{x}(k) \approx \frac{2x(k) - 5x(k+1) + 4x(k+2) - x(k+3)}{T_s^2}, \tag{29}$$

with a step size T_s, resulting in an accuracy of order $O(T_s)^2$, Fornberg (1988). Matching the form of (1), with $s=1$, $n=1$ and $T=4$ the shape matrix

$$\mathbf{V} = \begin{pmatrix} 2+(\omega^2T_s^2) & -5 & 4 & -1 \end{pmatrix} \tag{30}$$

can be used to evaluate, how close any given discrete-time signal matches the shape of a sinusoidal wave.

4.3 Constrained Active Power Filter Control

It is assumed that in a 50 Hz grid the measured disturbance of the current period is the same as the measured disturbance of the next period, i.e. harmonic distortion does not change in between periods. This allows for a periodic receding horizon strategy, where instead of updating the initial state and the optimization problem at every sampling step, the optimal input for a whole period is applied before updating the optimization problem. This allows for larger computation windows, since the new optimal input has to be calculated only every 0.02 s instead of every sampling step.

Using the sinusoidal shape matrix (30), the non-diagonal Hessian $\mathbf{Q_S}$ can be generated using the pattern band matrix $\mathbf{P_v}$ as shown in (22). Ultimately, the measured disturbance, that needs to be compensated such that the target signal assumes a sinusoidal shape, is incorporated into the dense LS^3 MPC optimization problem (7) with

$$\mathbf{P} = \boldsymbol{\Theta}^\intercal\mathbf{Q}_S\boldsymbol{\Theta} + \mathbf{R}, \tag{31}$$

$$\mathbf{q} = -2\boldsymbol{\Theta}^\intercal\mathbf{Q}_S\left(\boldsymbol{\Psi}\mathbf{x}(k) + \boldsymbol{\Upsilon}\mathbf{u}(k-1) + \boldsymbol{\Gamma}\mathbf{d}_m\right), \tag{32}$$

$$\mathbf{l} = \mathbf{x}_{\min} - \left(\boldsymbol{\Psi}\mathbf{x}(k) + \boldsymbol{\Upsilon}\mathbf{u}(k-1) + \boldsymbol{\Gamma}\mathbf{d}_m\right), \tag{33}$$

$$\mathbf{o} = \mathbf{x}_{\max} - \left(\boldsymbol{\Psi}\mathbf{x}(k) + \boldsymbol{\Upsilon}\mathbf{u}(k-1) + \boldsymbol{\Gamma}\mathbf{d}_m\right), \tag{34}$$

with

$$\boldsymbol{\Gamma} = \begin{pmatrix} \mathbf{E} & \mathbf{0} & \mathbf{0} & \cdots & \mathbf{0} \\ \mathbf{AE} & \mathbf{E} & \mathbf{0} & \cdots & \mathbf{0} \\ \vdots & \vdots & \vdots & \ddots & \\ \mathbf{A}^{H_p-1}\mathbf{E} & \mathbf{A}^{H_p-2}\mathbf{E} & \mathbf{A}^{H_p-3}\mathbf{E} & \cdots & \mathbf{E} \end{pmatrix}, \tag{35}$$

where $\mathbf{x}_{\max} \in \mathbb{R}^n$ denotes the maximum state constraint vector containing upper limits for each state and $\mathbf{x}_{\min} \in \mathbb{R}^n$ denotes the minimum state constraint vector containing lower limits for each state. The targeted state is the first state i_f, therefore only constraints for this state will be applied and the constraints for the second state i_c will be set to $\pm\inf$. With this formulation it is also possible to compute the unconstrained solution by setting $\mathbf{x}_{\max} = (\inf \ \inf)^\intercal$ and $\mathbf{x}_{\min} = (-\inf \ -\inf)^\intercal$, hence not constraining the solution space at all.

For the sparse formulation, the disturbance is incorporated into the problem with

$$\mathbf{c} = \begin{pmatrix} -\mathbf{A}\mathbf{x}(k) \\ -\mathbf{E}\mathbf{d}_m(k-H_p) \\ -\mathbf{E}\mathbf{d}_m(k-H_p+1) \\ \cdots \\ -\mathbf{E}\mathbf{d}_m(k-1) \end{pmatrix}, \tag{36}$$

where $(\mathbf{d}_m(k-H_p) \ \mathbf{d}_m(k-H_p+1) \ \cdots \ \mathbf{d}_m(k-1))^\intercal$ corresponds to the vector of measured disturbances of the previous period. The state constraints are simply applied setting the lower and upper bounds of the decision variable $\underline{\mathbf{z}}$ and $\overline{\mathbf{z}}$ to $\mathbf{x}_{\min}$ and $\mathbf{x}_{\max}$ appropriately.

4.4 Simulation Setup

Table 1 shows the parameters of the equivalent circuit used to model the application example.

Table 1. Parameters for the equivalent circuit shown in Fig. 1.

Transmission		Compensation Coupling		Internal Resistances	
R_1	L_1	R_2	L_2	R_3	R_4
1 Ω	10 μH	0.05 Ω	3.5 mH	10 kΩ	10 kΩ

For all simulation runs, diagonal input weighting matrices $\tilde{\mathbf{R}}$ are used with a common weighting factor of 10^{-7}.

The amount of harmonics contained in a waveform can be indicated by the total harmonic distortion (THD), which is defined as the ratio of the root mean square (RMS) value of the current harmonics and the fundamental current expressed in percentage as

$$\mathrm{THD} = \frac{\sqrt{\sum_{h=2}^{\infty} \left(I^{(h)}\right)^2}}{I^{(1)}} \cdot 100\,\% \,. \tag{37}$$

The periodic disturbance signal

$$i_{l0} = 10\sin(\omega_f t) + 5\sin(5\,\omega_f t) + 3\sin(7\,\omega_f t)\,, \tag{38}$$

with the angular frequency $\omega_f = 100\pi\ \mathrm{rad\,s^{-1}}$ is used to resemble the harmonic current drawn by a rectifier, which is a typical nonlinear load in the grid. The THD of this disturbance signal is 58.3 %.

As QP solver, the open-source tool OSQP is used, see Stellato et al. (2017), with a convergence tolerance set to $\epsilon = 10^{-8}$. All simulations are computed using MATLAB R2018b exclusively. Average computing times are determined by running the solver for an optimization problem for $N = 100$ times and calculating the mean of the run time for each solution. Numerical tests are executed on an Intel® Pentium® CPU G3260 @ 3.3 GHz, running Microsoft® Windows 10™.

4.5 Simulation Results

Fig. 2 shows the compensated feeder line current i_f using the condensed optimization problem formulation with sampling time $T_s = 0.2$ s, prediction horizon $H_p = 100$, input horizon $H_u = 100$, and state constraints set to $\pm\inf$, resulting in an unconstrained harmonic current compensation. In the first period, the disturbance is unknown and thus set to zero, so no compensation is taking place, while starting from the second period the harmonic current is being compensated by the controlled current i_{c0}, reaching a THD of 0.030 %.

Applying state constraints to the same MPC optimization leads to equally good compensation results while maintaining the upper and lower feeder line current constraints. This is a benefit over the unconstrained LS^3 MPC approach, where feeder line currents tend to increase or decrease over time, see Cateriano Yáñez et al. (2018). Fig. 3 shows feeder line currents, compensated with different state constraints.

Using the sparse optimization problem formulation also leads to compensated feeder line currents with notably faster solving times than when using the dense problem formulation. Faster computation times of the sparse formulations are expected due to the numerically exploitable

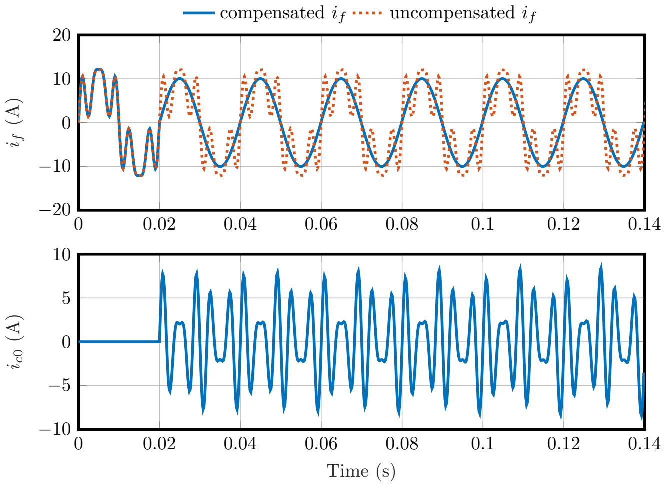

Fig. 2. Simulation of the system controlled with LS^3 MPC using the OSQP solver. No constraints are applied. The upper plot shows the feeder line current, the lower plot shows the compensation current.

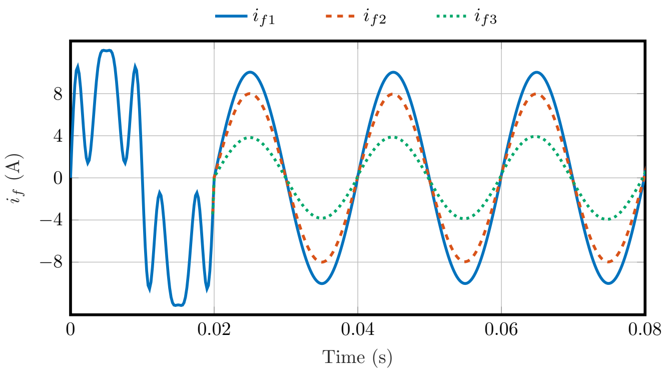

Fig. 3. Feeder line current compensation with different state constraints: i_{f1} shows the unconstrained compensated feeder line current, i_{f2} is constrained to ±8 A and i_{f3} is constrained to ±4 A.

pattern of the Hessian. With longer prediction horizons the computational benefit of sparse notations even grows as shown in table 2.

Table 2. Comparison of harmonic compensation with both sparse and condensed formulated LS^3 MPC optimization problems.

	THD with $T_s = 0.4$ ms $H_p = 50$, $H_u = 50$		THD with $T_s = 0.2$ ms $H_p = 100$, $H_u = 100$	
State limit	sparse	dense	sparse	dense
± inf A	0.123 %	0.124 %	0.021 %	0.030 %
±8 A	0.123 %	0.124 %	0.016 %	0.031 %
±6 A	0.122 %	0.101 %	0.005 %	0.031 %
±4 A	0.121 %	0.124 %	0.014 %	0.032 %
±2 A	0.117 %	0.125 %	0.075 %	0.036 %
±1 A	0.109 %	0.125 %	0.035 %	0.042 %
average solving time	0.17 ms	1.18 ms	0.33 ms	5.24 ms

The difference in THD reduction when comparing both optimization problem formulations is tied to the structure of the controller—while the sparse notation directly calculates the optimal input, the condensed notation calculates the optimal input change $\Delta\mathbf{U}$ as laid out in section 3. While the overall THD reduction shown in table 2 is similar when comparing both approaches, when using input changes the THD takes longer to reach a steady compensation current. Fig. 4 shows the evolution of the THD measured at the beginning of every period when using the direct input as well as the input change control approach. As can be seen, calculating the input i_{c0} directly decreases the THD immediately, while using input changes reaches the same THD reduction after several periods. Further investigations into the numerical properties for the cause of this effect is needed.

Using constrained LS^3 MPC for harmonic current compensation in the grid proved to be successful in simulations, but with this approach only lower and upper current bounds can be set. This strategy is sufficient for a device like the APF, that needs to maintain a sinusoidal signal shape while not exceeding certain bounds. When the control goal is to assume a sinusoidal signal shape with a specified amplitude magnitude, i.e. to compensate unbalanced voltages and to maintain a prescribed RMS voltage, this control method falls short, since there is no way to incorporate the amplitude magnitude into the optimization problem in a different way than setting upper and lower constraints. Formulating the cost function in such a way, that it includes information about the state signal RMS, addresses this issue, although this would lead to a biquadratic optimization problem. An approach to formulating this optimization problem is given in Cateriano Yáñez et al. (2020). Proving the convexity of this optimization problem and exploring possibilities to efficiently solve this problem need to be investigated further.

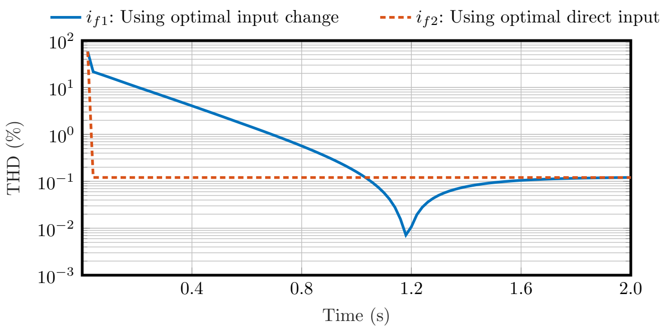

Fig. 4. Evolution of the THD for the compensation solution using condensed and sparse problem formulations.

The successful implementation of this approach relies heavily on the efficiency of the QP solver. The discussed approach is expected to be on the edge of the computational capabilities of today's high-end microcontrollers, such that highly efficient programming is needed; or eventually, FPGA programming will be necessary.

5. CONCLUSION

Shape classes can be used for linear state signal shaping MPC, i.e. controlling a plant in such a way, that the states assume a given shape signal. Contrary to reference tracking MPC, where the reference signal is tied to a specific time or sample step and the tracking error is minimized, the wanted signal shape is incorporated into the state weighting matrix and the shape residual is minimized. The only difference to a regular MPC optimization problem is the non-diagonal state weighting matrix, thus constraints and commonly used QP solvers can be used. In an application example, this concept is illustrated by a simulated control of an active power filter. A harmonic shape class is used to compensate harmonics in an electrical grid and to provide pure sinusoidal feeder line currents, reducing the total harmonic distortion to very low amounts.

REFERENCES

Brandonisio, F. and Kennedy, M.P. (2014). *Noise-Shaping All-Digital Phase-Locked Loops: Modeling, Simulation, Analysis and Design*. Analog Circuits and Signal Processing. Springer International Publishing.

Cateriano Yáñez, C., Lichtenberg, G., Pangalos, G., and Sanchis Sáez, J. (2020). An approach to state signal shaping by limit cycle model predictive control. In *2020 IFAC World Congress*. Submitted.

Cateriano Yáñez, C., Pangalos, G., and Lichtenberg, G. (2018). An approach to linear state signal shaping by quadratic model predictive control. In *2018 European Control Conference (ECC)*.

Egerstedt, M. and Hu, X. (2001). Formation constrained multi-agent control. *IEEE Transactions on Robotics and Automation*, 17(6), 947–951.

Fornberg, B. (1988). Generation of finite difference formulas on arbitrarily spaced grids. *Mathematics of computation*, 51(184), 699–706.

Fuchs, E.F. and Masoum, M.A.S. (2015). *Power Quality in Power Systems and Electrical Machines*. Elsevier, Amsterdam.

Jerez, J.L., Kerrigan, E.C., and Constantinides, G.A. (2012). A Sparse and Condensed QP Formulation for Predictive Control of LTI Systems. *Automatica*, 48(5), 999–1002.

Kumar, P. and Mishra, M.K. (2016). A Comparative Study of Control Theories for Realizing APFs in Distribution Power Systems. In *2016 National Power Systems Conference (NPSC)*, 1–6.

Lu, H., Kearney, M., Li, Y., Liu, S., Daniel, W.J.T., and Meehan, P.A. (2016). Model predictive control of incremental sheet forming for geometric accuracy improvement. *The International Journal of Advanced Manufacturing Technology*, 82(9), 1781–1794. doi: 10.1007/s00170-015-7431-5.

Maciejowski, J.M. (2002). *Predictive Control: With Constraints*. Prentice Hall, Harlow [u.a.].

Stellato, B., Banjac, G., Goulart, P., Bemporad, A., and Boyd, S. (2017). OSQP: An Operator Splitting Solver for Quadratic Programs.

Weihe, K., Cateriano Yáñez, C., Georg Pangalos, and Lichtenberg, G. (2018). Comparison of Linear State Signal Shaping Model Predictive Control with Classical Concepts for Active Power Filter Design. In *Proceedings of 8th International Conference on Simulation and Modeling Methodologies, Technologies and Applications*, 176–174. Porto.